ACADEMIC PRESS

Available online at www.sciencedirect.com

SCIENCE DIRECT®

VIROLOGY

Virology 312 (2003) 270–280

www.elsevier.com/locate/yviro

Enzymatic activities of the GB virus-B RNA-dependent RNA polymerase

C.T. Ranjith-Kumar,[a] Jan Lee Santos,[a] Lester L. Gutshall,[b] Victor K. Johnston,[b] Juili Lin-Goerke,[b] Min-Ju Kim,[a] David J. Porter,[c] Derrick Maley,[b] Cathy Greenwood,[d] David L. Earnshaw,[d] Audrey Baker,[d] Baohua Gu,[b] Carol Silverman,[d] Robert T. Sarisky,[b] and Cheng Kao[a,1,*]

[a] *Department of Biology, Indiana University, Bloomington, IN 47405, USA*
[b] *Department of Virology, GlaxoSmithKline Pharmaceuticals, Collegeville, PA 19426, USA*
[c] *Department of Bioanalytical Pharmacology, The Metabolic and Viral Diseases Center of Excellence for Drug Discovery, GlaxoSmithKline Pharmaceuticals, Collegeville, PA 19426, USA*
[d] *Discovery Research, GlaxoSmithKline Pharmaceuticals, Collegeville, PA 19426, USA*

Received 26 November 2002; returned to author for revision 3 January 2003; accepted 13 March 2003

Abstract

The GB virus-B (GBV-B) nonstructural protein 5B (NS5B) encodes an RNA-dependent RNA polymerase (RdRp) with greater than 50% sequence similarity to the hepatitis C virus (HCV) NS5B. Recombinant GBV-B NS5B was reported to possess RdRp activity (W. Zhong et al., 2000, J. Viral Hepat. 7, 335–342). In this study, the GBV-B RdRp was examined more thoroughly for different RNA synthesis activities, including primer-extension, de novo initiation, template switch, terminal nucleotide addition, and template specificity. The results can be compared with previous characterizations of the HCV RdRp. The two RdRps share similarities in terms of metal ion and template preference, the abilities to add nontemplated nucleotides, perform both de novo initiation and extension from a primer, and switch templates. However, several differences in RNA synthesis between the GBV-B and HCV RdRps were observed, including (i) optimal temperatures for activity, (ii) ranges of Mn^{2+} concentration tolerated for activity, and (iii) cation requirements for de novo RNA synthesis and terminal transferase activity. To assess whether the recombinant GBV-B RdRp may represent a relevant surrogate system for testing HCV antiviral agents, two compounds demonstrated to be active at nanomolar concentrations against HCV NS5B were tested on the GBV RdRp. A chain terminating nucleotide analog could prevent RNA synthesis, while a nonnucleoside HCV inhibitor was unable to affect RNA synthesis by the GBV RdRp.

Keywords: GBV-B; HCV; RNA-dependent RNA polymerase

Introduction

An estimated 2–3% of the world's human population is chronically infected with hepatitis C virus (HCV) that causes significant liver disease that can eventually lead to the development of hepatocellular carcinoma (World Health Organization, 1998; Alter and Mast, 1994). The limited availability of and high cost associated with studies using large nonhuman primates limits our understanding of HCV biology and clinical management of this disease. The GB virus-B (GBV-B) is a single-stranded positive-sense RNA virus and is closely related to HCV, another member in the family *Flaviviridae*. GBV-B is proposed to provide a small animal model for hepatitis in *Saguinus* species (tamarins) (Muerhoff et al., 1995; Simons et al., 1995), although it is not clear whether GBV can be a substitute system for studies of HCV replication.

* Corresponding author. Fax: +1-979-845-9274.
E-mail address: ckao@bbserv.tamu.edu (C. Kao).
[1] Present address: Department of Biochemistry and Biophysic, 2128 TAMU, Texas A&M University, College Station, TX College Station, Texas 77843-2128.

0042-6822/03/$ – see front matter © 2003 Elsevier Science (USA). All rights reserved.
doi:10.1016/S0042-6822(03)00247-2

GBV-B was isolated from tamarins inoculated with a blood sample from a surgeon (G.B.) suffering from acute hepatitis (Deinhardt et al., 1967). GBV-B causes acute, self-limited hepatitis in tamarins, evidenced by a rise in serum alanine transaminase level (Schaluder et al., 1995a, b). Although the acute nature of GBV-B infection in tamarins distinguishes this hepatitis from HCV infection in humans, the polyproteins from both viruses share approximately 25 to 30% similarity at the amino acid level (Muerhoff et al., 1995), and studies using chimeric HCV and GBV-B NS3 proteins have demonstrated functional similarities (Butkiewicz et al., 2000). Moreover, the coding region for GBV-B nonstructural protein 5B (NS5B) and the HCV NS5B have 37% identity and 52% similarity of amino acids residues (Muerhoff et al., 1995). The GBV-B NS5B protein was recently purified and shown to possess RNA-dependent RNA polymerase (RdRp) activity (Zhong et al., 2000b), a function previously confirmed for HCV and BVDV NS5Bs (Behrens et al., 1996; Zhong et al., 1998). These studies stimulated speculation that GBV-B NS5B may provide a useful target to test inhibitors of the HCV RdRp. It is therefore useful to characterize the activities of the GBV-B RdRp.

Recombinant NS5B proteins from several members of the *Flaviviridae* have been demonstrated to possess a number of activities. These include the ability to (1) add non-templated nucleotide(s) to the 3′ hydroxyl of a template (Behrens et al., 1996; Ranjith-Kumar et al., 2001); (2) extend from a template primed with an oligonucleotide (Behrens et al., 1996; De Francesco et al., 1996; Lohmann et al., 1997, 1998); (3) initiate RNA synthesis using a single-nucleotide as the primer, also known as de novo initiation (Kao et al., 1999, 2000; Luo et al., 2000; Oh et al., 2000; Shim et al., 2002); (4) synthesize a product using two or more noncovalently linked templates in a mechanism called template switching (Kim and Kao, 2001); (5) preferentially use Mn^{2+} for efficient de novo initiation and Mg^{2+} for primer-extension (Ranjith-Kumar et al., 2002b). In this work, we examined the biochemical activities of the GBV-B RdRp to determine how its activities compare to the other recombinant RdRps.

Results and discussion

GBV-B RdRp purification

The carboxy-terminal 23 amino acids of the GBV-B polymerase were removed and replaced with six histidines to facilitate solubility and protein purification. Purification with nickel column chromatography resulted in an eluate of ~90% purity which was subsequently purified using poly(U) resin. The resulting preparation contained only the protein of the expected size with approximate purity of >97% (Fig. 1A). Mass spectroscopy revealed that the purified protein was within 1 Da of the mass for the GBV-B protein if the N-terminal methionine was removed, a common processing event for recombinant proteins expressed in *Escherichia coli.* The protein also reacted with a polyclonal serum generated from a peptide made from the GBV-B RdRp sequence (Fig. 1A, lane W). These results demonstrate that the GBV-B NS5B protein is of a quality suitable for biochemical analysis.

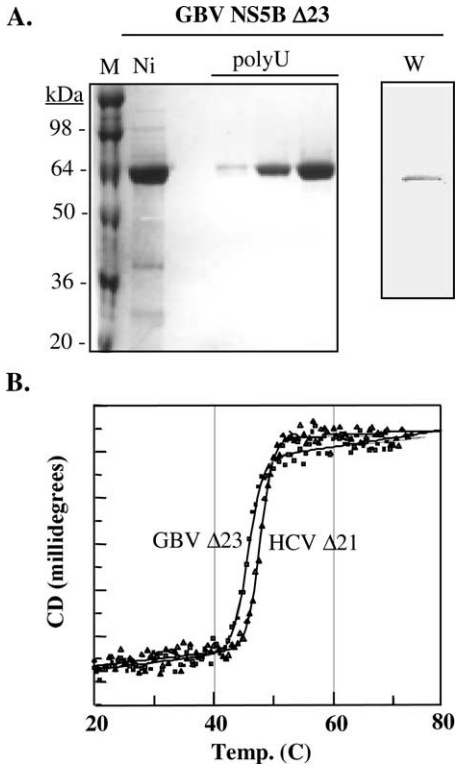

Fig. 1. Expression, purification, and CD spectral analysis of the GBV-B NS5B. (A) A 10% SDS–PAGE stained with Coomassie blue. Lane 1, molecular weight marker whose sizes in kilodaltons (kDa) are indicated to the left of the image of the gel. The lane labeled Ni is from the peak fraction of a Talon affinity column. The three lanes labeled poly(U) contain three fractions from a poly(U) column that were pooled for the RNA synthesis assays. W identifies a lane from a Western blot using antisera to a peptide synthesized from the GBV-B sequence to probe the proteins eluted from a Talon column. (B) Thermal denaturation study of the GBV-B and HCV RdRps. The HCV and GBV-B RdRps were at 2.4 and 3.1 μM, respectively. The proteins were in a buffer consisting of 20 mM Tris, 25 mM KCl, 3.2 mM DTT, 7.5 mM $MgCl_2$, 0.37 mM NaCl, 1% glycerol pH 7.5. Data were fitted to an equation for a two-state unfolding model. T_m values for GBV-B and HCV were 47.75 ± 0.07 and 48.06 ± 0.07°C, respectively. The CD signal at 220 nM was determined from 20 to 75°C.

To assess how the secondary structure of the GBV RdRp compares to the HCV RdRp, CD spectroscopy was performed. The CD spectra of both the GBV-B (Δ23) and the HCV (Δ21) RdRps showed that both were predominantly α-helical in secondary structures. Furthermore, both have similar melting points, with the GBV-B and HCV RdRp losing half of their secondary structure at 48.1 and 47.8°C, respectively (Fig. 1B). Given the degree of conservation in the two proteins, the similarities in the spectral and thermodynamic properties of the two proteins were to be expected.

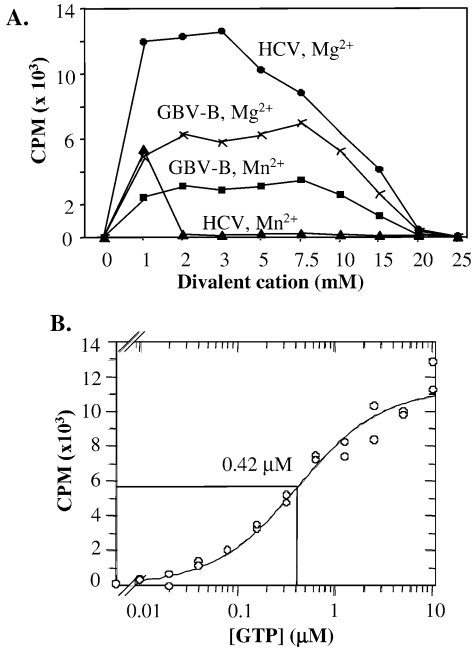

Fig. 2. Properties of the GBV-B RdRp characterized using a primer-extension assay. (A) A comparison of the effects of increasing Mg^{2+} and Mn^{2+} concentrations on RNA synthesis by the HCV and GBV-B RdRps. The reactions containing 10 nM NS5B, 256 nM primer-template, 20 mM Tris–HCl pH 7.5, 25 mM KCl, 3 mM dithiothreitol, and variable concentrations of divalent metal were incubated for 1 h at 25°C in the presence of varying amounts of [α-^{33}P]GTP. (B) Determination of the K_M for GTP. Polymerase reactions performed with the same buffer conditions as in (A), with $MgCl_2$ at a final concentration of 7.5 mM. The reactions were performed in a streptavidin-coated FlashPlate as described under Materials and methods. The K_M of 0.42 μM was derived from the midpoint of the assay.

Primer extension by the GBV-B RdRp

Primer-extension activity of the GBV-B RdRp was assayed by monitoring the incorporation of [^{33}P]-rGTP into an oligo(rG_{13}) primed poly(rC) RNA. Using this assay, we examined how reaction conditions affect nucleotide polymerization. Since polymerases are metal-dependent enzymes, and the activities of the HCV RdRp are affected by divalent metal (Ranjith-Kumar et al., 2002a,b), we assessed whether different concentrations of the divalent metals Mg^{2+} or Mn^{2+} could be used for template-dependent GTP incorporation. The GBV RdRp was purified in a buffer that lacked divalent metal. In the absence of poly(C) or exogenously provided divalent metal, no radiolabel incorporation was observed (Fig. 2A). However, addition of either Mg^{2+} or Mn^{2+} increased RNA synthesis. Both the HCV and the GBV RdRps exhibited high activities over a broad range of Mg^{2+}, with the peaks being at 3 and 7.5 mM, respectively. In the presence of a range of Mn^{2+} from 1 to 7.5 mM, the GBV-B RdRp exhibited activity, with higher concentrations becoming inhibitory (Fig. 2A). However, consistent with previous studies (Lohmann et al., 1998), ~1.0 mM $MnCl_2$ was the optimal for the HCV NS5B; RNA synthesis was reduced by 90% when greater than 3 mM $MnCl_2$ was added to the reaction. Contrary to the results of Zhong et al., (2000b), we found that Mn^{2+} is not specifically required for RNA synthesis by the GBV-B RdRp since reactions with Mg^{2+} as the only divalent metal were capable of efficient RNA synthesis. In addition, RNA synthesis was consistently higher in reactions with Mg^{2+} than with Mn^{2+}.

Given that Mg^{2+} is likely to be the most relevant metal for RNA synthesis in a virus-infected cell, we determined the K_M for GTP incorporation using the primer-extension assay. In the presence of 7.5 mM Mg^{2+}, the K_M for GTP was 0.42 μM (Fig. 2B), similar to the previously reported value of 0.54 μM for the HCV RdRp (Lohmann et al., 2000).

Additional requirements of the GBV-B RdRp in primer extension were examined, including the effects of pH, monovalent and divalent cations, and the incubation temperature (Fig. 3A). For the GBV-B RdRp, RNA synthesis at 37°C was approximately half of that at 25°C (data not shown). In contrast, the HCV RdRp was more active at 37°C than at 25°C (Fig. 3A and also Ferrari et al., 1999). Both HCV and GBV-B polymerases had peak RNA synthesis activities between pH 7.3 and 7.5 in a Tris buffer, and both had significantly decreased RNA synthesis at KCl concentrations higher than 50 mM (Fig. 3A).

To examine whether the concentration of the GBV-B RdRp affects primer extension, assays were performed for 1 h using 2, 5, 10, 20, 30, 40 and 50 nM of the GBV-B

A.

	Optimal		Acceptable*	
Condition	GBV-B	HCV	GBV-B	HCV
pH	7.4	7.4	6-8	6-8
$MgCl_2$ (mM)	7.5	4.0	5-10	2-5
$MnCl_2$ (mM)	7.5	<1.0	2.5-10	1-3
Temp (°C)	25	37	20-35	20-45
Na or K(mM)	<12.5	<12.5	0-50	0-50

* Range in which RNA synthesis is >20% of optimal.

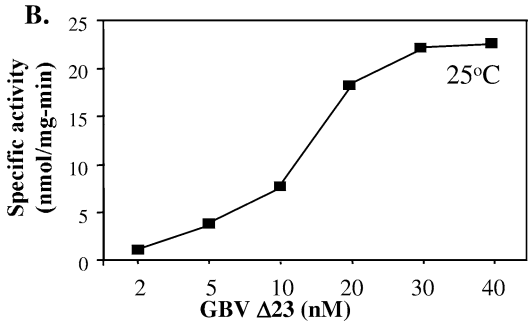

Fig. 3. Conditions for RNA synthesis by the GBV-B and HCV RdRps. (A) Summary of the conditions optimal for primer extension from a poly(C) template and oligonucleotide G primer under a variety of reaction conditions. Titrations of the different conditions were performed using the streptavidin flash plate assay. (B) Effects of increasing GBV RdRp concentration on RNA synthesis at 25°C. Reactions at each time point were performed for 1 h using the Flashplate assay.

RdRp. At 25°C, a 20-fold increase in the GBV RdRp concentration resulted in a ~23-fold increase in the specific activities (Fig. 3B). However, the increase was nonlinear, with the greatest increase in activity at the protein concentrations between 10 and 30 μM (Fig. 3B). The nonlinear increase in RNA synthesis demonstrates that higher concentrations of the GBV RdRp are preferred for productive RNA synthesis, a feature consistent with the observations of HCV RdRp (Wang et al., 2002). However, we cannot unambiguously conclude whether or not oligomerization of the GBV-B is required for RNA synthesis.

De novo initiated RNA synthesis

Although the HCV and GBV-B RdRps are capable of initiating RNA synthesis in a primer-dependent manner, a de novo mechanism is likely to be the mode of initiation by flaviviruses in cells (Kao et al., 2001). In a de novo initiation assay, the template initiation nucleotide, a cytidylate, is specifically recognized (Kim et al., 2000; Ranjith-Kumar et al., 2002a). To determine whether the GBV RdRp can initiate RNA synthesis by a de novo mechanism, we used an RNA named LE19 (Fig. 4A). Monomers of LE19 exist in dynamic equilibrium with a dimer that is formed through six 3-base pairs between two LE19 molecules. The primer-extension product should generate a 32-nt product, as was observed (Fig. 4A and B). A 19-nt product consistent with de novo initiation was observed in reactions containing all four NTPs whether the reaction contained both 4 mM Mg^{2+} and 1 mM Mn^{2+}, or only 4 mM Mg^{2+} (Fig. 4B, lanes 1 and 3). In reactions with only CTP, we observed a labeled 20-nt product that is due to nontemplated nucleotide addition (Fig. 4B, lane 2). This activity will be addressed in the section below.

To determine whether the GBV-B RdRp is capable of de novo initiation, we used a version of LE19 named LE19P, wherein the 3′-terminus was modified with a puromycin, which allows de novo initiation but prevents primer extension. The 19-nt de novo initiated RNA was observed with LE19P (Fig. 4B, lanes 5 and 7), thus proving that de novo initiation does take place. In addition, de novo initiation occurred whether Mn^{2+} was present or not. In fact, 1 mM Mn^{2+} decreased de novo initiation by the GBV-B RdRp by 30–50%. This result contrasts with that from the HCV RdRp, where Mn^{2+} increased de novo RNA synthesis by more than sevenfold (Ranjith-Kumar et al., 2002b). These results demonstrate that the GBV RdRp is able to initiate RNA synthesis by a de novo mechanism but with different divalent metal requirements from the HCV RdRp.

The effect of divalent metals on de novo initiation by the GBV-B RdRp was examined further (Fig. 5A). As expected, reactions with Mg^{2+} and Mn^{2+} directed significant synthesis levels of both de novo initiated and primer-extension products of 19- and 32-nt, respectively. Of the other metals tested, Ca^{2+}, Co^{2+}, Cu^{2+}, Ni^{2+}, and Zn^{2+}, there was no synthesis with the latter three metals. However, the reaction

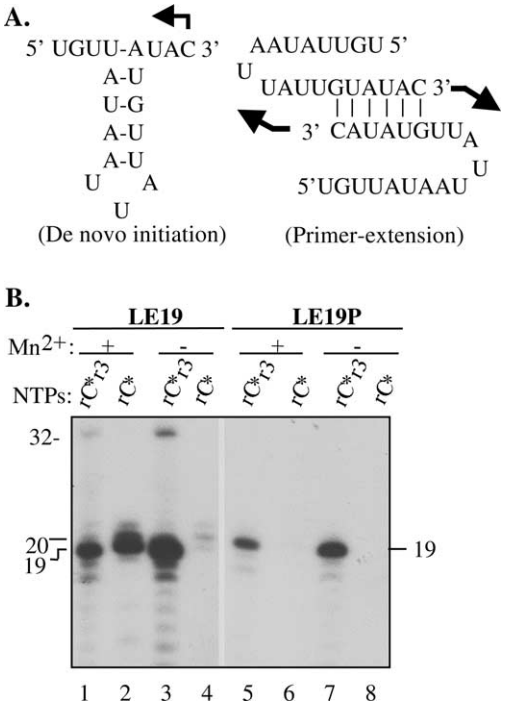

Fig. 4. De novo initiation of RNA synthesis by the GBV-B RdRp. (A) Schematic for the two conformations of LE19 that could lead to de novo initiation and primer extension. The arrows indicate the directions of RNA synthesis. (B) RNA synthesis from LE19 and LE19 modified with a 3′ puromycin. The NTPs used in each reaction are indicated above the autoradiogram. [α-^{32}P-]CTP is indicated as rC* and where the other three NTPs were used, they are indicated as r3. If the reaction contained 1 mM Mn^{2+}, it is denoted by a + in the Mn^{2+} column. Positions of the 19- and 32-nt de novo initiated and primer-extended products are shown next to the autoradiogram. The 20-nt RNA is the product due to the addition of a terminal nucleotide to the 3′-terminus of LE19.

with 10 mM of Ca^{2+} produced a low level of primer extension, while the one with 1 mM of Co^{2+} produced a low level of de novo initiation (Fig. 5A). Mg^{2+} at 10 mM final concentration has a slight inhibitory effect on the GBV RdRp, reducing the synthesis of the 19-nt RNA to 68% (Fig. 5C). Reactions with 10 mM Mn^{2+} were reduced in RNA synthesis by the GBV-B RdRp to less than 20% in comparison to the reaction with 1 mM Mg^{2+} (Fig. 5C). Last, the effects of Mg^{2+} and Mn^{2+} on primer extension and de novo initiation with LE19 are generally consistent with the results for metal requirements during primer extension from a ribo(C) template and oligo(G) primer.

To confirm the results concerning the requirements for divalent metal, we used a second RNA that could direct only de novo initiation with an RNA named 14-1 (Fig. 5B), which was previously characterized to produces a 14-nt initiated product (Kim and Kao, 2001). Unlike LE19, 14-1 can not efficiently produce a primer-extension product, but can direct template switch (Kim and Kao, 2001). Only the reactions with Mg^{2+} and Mn^{2+} were able to produce the expected 14-nt product, with some presumed prematurely terminated product being especially prominent in the reac-

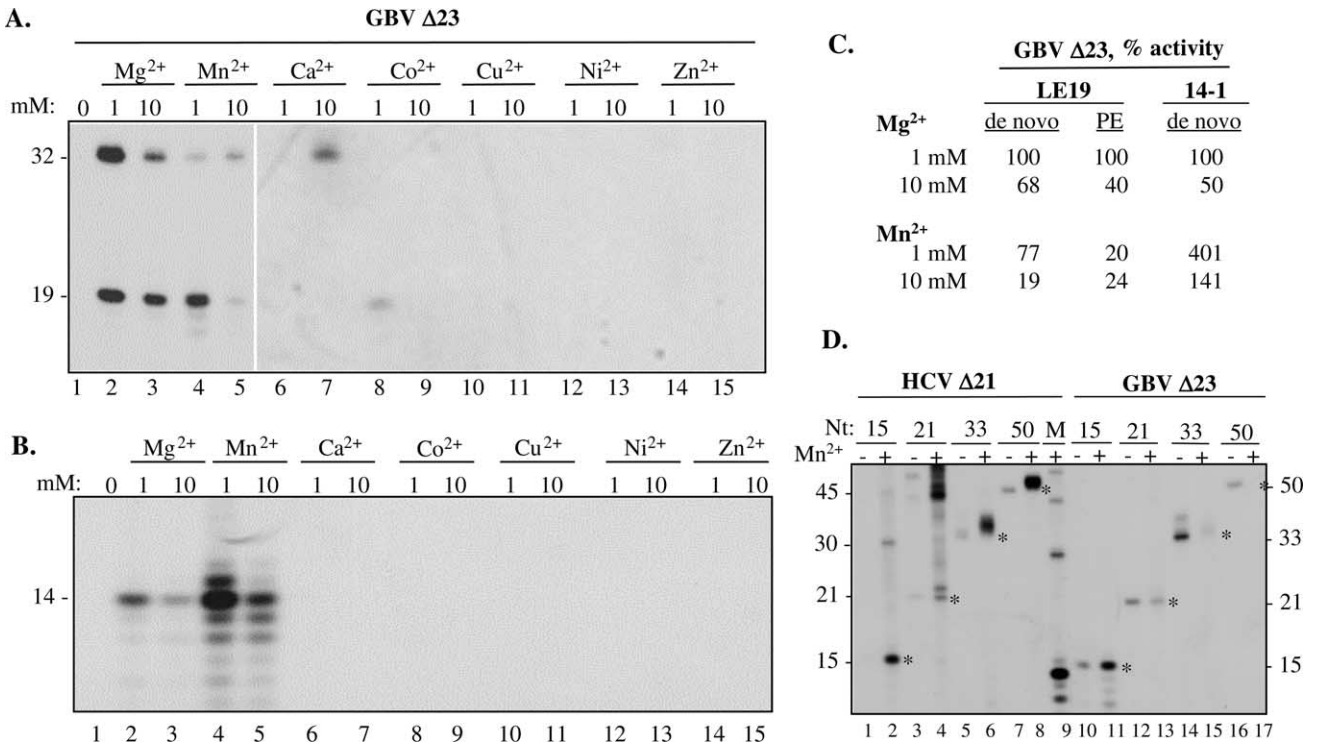

Fig. 5. Conditions required for de novo initiation of RNA synthesis by the GBV-B RdRp. (A) RNA synthesis from LE19 in the presence of 1 or 10 mM of different divalent metals. The GBV-B RdRp was prepared in the absence of any divalent metals in the buffer. The identity and final concentrations of different divalent metals are indicated above the autoradiogram. The positions of the 19 and 32-nt de novo initiated and primer-extended products are indicated to the left of the autoradiogram. (B) RNA synthesis from template 14-1 in the presence of 1 or 10 mM of different divalent metals. (C) Quantification of the amount of de novo initiated or primer-extended products made by the GBV-B RdRp in the presence of Mg^{2+} or Mn^{2+}. The percent of RNA synthesis is normalized to the activity observed in the reaction with 1 mM Mg^{2+}, which is taken as 100%. (D) A correlation between the length of the template and the effects of Mn^{2+} on de novo initiated RNA synthesis by the HCV and GBV-B RdRps. The names of the templates denote their length. All of the templates share an initiation cytidylate at the 3′-terminus. The molecular weight marker is made from RNA 14-1 (lane 9, also marked at the top of the autoradiogram with M) generates a multimer of 14-nt products that was previously characterized in Kim and Kao (2001). The asterisks identify the de novo initiated products.

tion with Mn^{2+}. Relative quantification of the products from 14-1 is in Fig. 5C.

In comparing the results from LE19 and 14-1, there was a notable difference in the amounts of de novo initiated products made in the reactions containing Mg^{2+} and Mn^{2+}. Production of the de novo initiated products from 14-1, but not LE19, was stimulated several fold with Mn^{2+}. This indicates that at least some of the effect of Mn^{2+} is on template usage by the GBV-B RdRp. To examine whether there is a correlation between characteristics of the template and the effects of Mn^{2+}, several templates between 15 and 50 nt were tested. All of these that contain an initiation cytidylate as part of a single-stranded sequence, a feature which was demonstrated to be conducive for de novo initiation (Kao et al., 2000). The reactions were performed with 4 mM Mg^{2+}, and both 4 mM Mg^{2+} and 1 mM Mn^{2+}. For the HCV RdRp, having Mn^{2+} in the reaction increased the amount of de novo initiated products from all of these templates (Fig. 5D, see products denoted with asterisks). In contrast, in the reactions with GBV-B RdRp, only the 15-nt product was increased in the presence of Mn^{2+} (Fig. 5D, compare lanes 10 and 11). Synthesis of the de novo initiated products from longer templates were inhibited by Mn^{2+}, with the degree of inhibition increasing with the length of the template. These results provide an explanation for the apparently discrepant results in Figs. 5A and B and suggest that the Mn^{2+}-dependent effect on de novo initiation is dependent on the length of the template. Additional analysis is needed to understand the mechanism of this effect.

Terminal nucleotide addition by the GBV-B RdRp

Some faint products longer than the length expected from the template were observed in the de novo initiation reactions (e.g., Figs. 4B and 5B). These products could arise by terminal nucleotide addition to the template and/or to the nascent RNA. Consistent with this hypothesis, the 20-nt product in a reaction containing only the radiolabeled CTP (Fig. 4B, lanes 2 and 4) was not seen with LE19P, which lacks a 3′ hydroxyl and prevents nontemplated nucleotide addition (Fig. 4B, lanes 6 and 8). These reactions demonstrate that the GBV-B RdRp has terminal nucleotidyl transferase (TNTase) activity.

The HCV RdRp could preferentially incorporate either AMP or CMP to the end of the template, depending on the template sequence (Ranjith-Kumar et al., 2001). To exam-

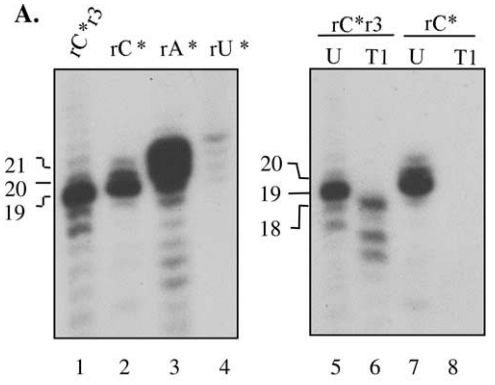

B.

Template	Sequence (5' to 3')	CMP/AMP incorporation
14-1	AAAUCCUCUGAUAC	0.4
14-2	AA**CCUUAC**UGAUAC	0.8
14-3	**CCAUU**CUCUGAUAC	0.6
14-16	AAAUCCUCUGAUA**U**	1.7
14-17	AAAUCCUCUGAUA**A**	0.03
14-18	AAAUCCUCUGAUA**G**	0.84
14-19	AAAUCCUCUGAU**UC**	0.14
14-21	AAAUCCUCUG**UUAC**	0.13
14-22	AAAUCCUCU**C**AUAC	0.04

Fig. 6. Template requirements for TNTase activity. (A) Left panel, use of different radiolabeled NTPs for terminal nucleotide addition to the 3′-terminus of LE19. Right panel, demonstration that the labeled RNAs contain a terminally added nucleotide. Reactions untreated (U) or treated with RNase T_1 (T1) are indicated above the autoradiogram. An asterisk (*) identifies the radiolabeled nucleotide. r3 denotes reactions performed in the presence of nonradiolabeled GTP, ATP, and UTP. The lengths of the reaction productions are indicated to the side of the autoradiograph. (B) Examination of the effects of the template sequence on the terminal addition of cytidylate or adenylate. The nucleotides changed in the templates are indicated in bold letters.

ine the requirements with the GBV-B RdRp, reactions were performed with LE19 and either the α-^{32}P-radiolabeled rCTP, rATP, or rUTP (Fig. 6A). Of the three nucleotides tested, addition to the input template was highest with rATP (Fig. 6A, lane 3), then with rCTP (lane 2), but barely detectable with rUTP (lane 4). To confirm that the nucleotides are added to the 3′ end of the template, RNase T1 digestions were performed on products of TNTase and RNA synthesis reactions to cleave the phosphodiester bond 3′ of a guanylate. Digestion of the newly synthesized RNA synthesized by GBV-B should yield an 18-nt RNA. This was observed in Fig. 6A, lane 6. Should the template LE19 become labeled by TNTase activity, the 18-nt RNA should not be observed. Instead, the largest labeled product should be 6-nt-long and migrate at the dye front with the unincorporated label. We did not observe the 18-nt RNA from the putative TNTase activity, consistent with our conclusion that the GBV-B RdRp has TNTase activity (Fig. 6A, lane 8).

The identity of nucleotides added terminally by the HCV RdRp is affected by template sequence (Ranjith-Kumar et al., 2001). Previously, RNA LE19 and LE19 with the 3′ cytidylate replaced with a guanylate have different abilities to accept nontemplated nucleotides, indicating that the RNA template sequence will regulate TNTase activity of the RdRp (Ranjith-Kumar et al., 2001). We used a series of 14-nt RNAs containing changes preferentially localized at the 5′ and 3′ ends to examine the effects of the TNTase activity of the GBV-B RdRp. The amount of AMP and CMP incorporation was determined, and the ratios are shown in Fig. 6B. All RNAs except 14–16 incorporated AMP more efficiently than CMP, suggesting that changes in template sequence and/or structure affect the efficiency of terminal nucleotide addition. Furthermore, a change of the 3′C to a G in template 14–18 resulted in a two-fold improvement in incorporation efficiency. This data are consistent with previous observations with the HCV RdRp that a change of the 3′-terminal nucleotide of RNA altered the preference of the terminally incorporated nucleotide (Ranjith-Kumar et al., 2001). However, the template sequence had different effects on the addition of the nontemplated nucleotide in comparison to the HCV RdRp; with RNA 14-1, the HCV RdRp preferentially incorporated CMP threefold more efficiently than AMP (Ranjith-Kumar et al., 2001), while the GBV-B incorporated CMP at only a fraction of the amount of AMP incorporated (Fig. 6B).

Template switch by the GBV-B RdRp

The BVDV and HCV RdRps can make product RNAs that are multimers of the length of the template. This is achieved by not terminating RNA synthesis at the end of a template RNA. Instead, the ternary complex uses additional template(s) to continue RNA synthesis (Kim and Kao, 2001). Template switch was previously examined with template (−)21dd, which allows de novo initiation but, due to the chemically synthesized (−)21dd possessing a 3′ dideoxycytidylate as the 3′-most nucleotide, neither primer extension nor the ligation of two or more templates (Kim and Kao, 2001). Hence, products that are dimeric or trimeric in length can be generated only by a template switch mechanism (Kim and Kao, 2001). For the BVDV RdRp, the dimeric RNA synthesized from (−)21dd was ~10% of the monomer (Kim and Kao, 2001). However, the GBV RdRp had a lower frequency of template switch, with only about 2% of the monomers, after normalizing for radiolabeled incorporation. Another expectation of the production of template-switch process is an increase in multimeric products with template concentrations. We tested for RNA synthesis by GBV-B RdRp with increasing concentrations of (−)21dd (Fig. 7A). RNA synthesis was observed only in the presence of all four NTPs (data not shown). Furthermore, both monomeric- and dimeric-length products were observed when the template was present at 12.5 nM. When the template was increased to 62.5 nM, trimer-length product was observed. These results suggest that the GBV-B RdRp could switch templates in vitro.

To demonstrate further that the GBV RdRp could switch

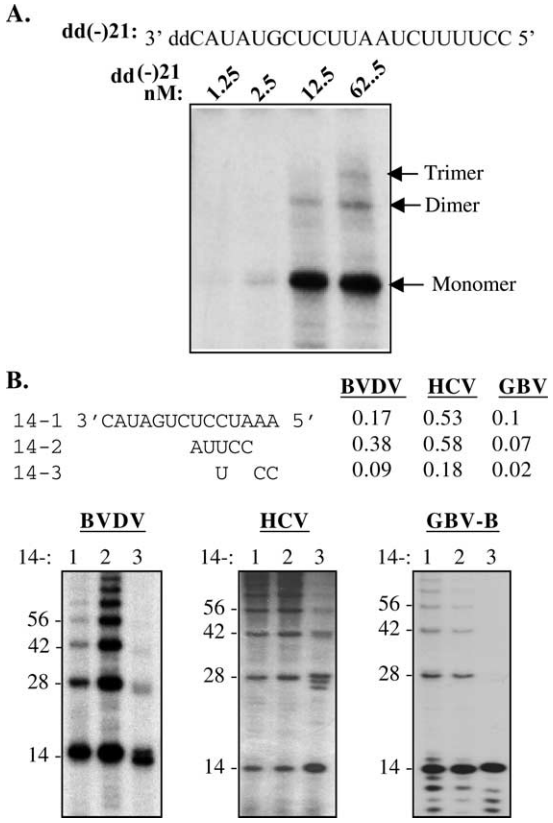

Fig. 7. Template switch by the GBV-B RdRp. (A) Demonstration that template switch requires higher template concentrations. The sequence of the chemically synthesized template used is shown above the autoradiogram. The 3′-terminal cytidylate is a dideoxynucleotide, which prevents primer extension and the ligation of two or more templates. The arrows beside the autoradiogram indicate the positions of the dimeric and trimeric products synthesized by the GBV-B RdRp. (B) Characterization of template switch by three viral RdRps using three templates that vary in their 5′sequence. Templates 14-1, 14-2, and 14-3 were previously used in the characterization of template switch by the BVDV RdRp and only the nucleotides in 14-2 and 14-3 that are different from 14-1 are shown. A portion of the autoradiogram of template switch by the BVDV was previously published in Kim and Kao (2001). The ratio of the dimeric to monomeric products is shown next to the sequence of the templates.

templates, we used a series of three RNAs that were previously characterized for their frequency of template switch by the BVDV RdRp (Fig. 7B) (Kim and Kao, 2001). Templates 14-1 and 14-2 were competent for high levels of template switch that resulted in a ladder of RdRp products that are multimers of 14-nt, while template 14-3 was much less efficient in inducing template switch, due to a change in the last two nucleotides at the 5′-terminus from adenylates to cytidylates (Fig. 7B). The pattern of template switch by the GBV-B RdRp generally followed trends seen with the BVDV and HCV RdRps, with multimers being observed with 14-1 and 14-2 and less abundant amounts of putative switch products with 14-3. Altogether, these results demonstrate that the GBV-B RdRp will, at some frequency, not terminate RNA synthesis at the 5′-terminus of the template and, instead, will use one or more additional templates for the continuation of elongative RNA synthesis. However, there are variations in the amount of dimeric RNAs made by the three RdRps relative to the monomers, indicating an inherent difference in the ability of each RdRp to perform a switch.

Template specificity of the GBV-B RdRp

Viral RNA replication in the infected cell needs to specifically recognize the viral template. Specificity could be attained in a number of ways, including the cotranslation of the viral proteins with the template to be used for replication, or by the recognition of specificity determinants in the viral RNA (Buck, 1996; Kao, 2002). The ability of the GBV-B RdRp to use a range of different templates for RNA synthesis portends that template specificity, except for the 3′-most initiation pyrimidine, is not determined solely by the recombinant RdRp. Instead, the viral replication complex and/or the process of assembling the replicase determines template specificity. This is also the situation claimed for the HCV RdRp (Kao et al., 2000; Luo et al., 2000; Zhong et al., 2000a). However, several groups have observed more specific recognition for one or more elements in the viral RNA (Oh et al., 2000; Kashiwagi et al., 2002). We examined whether the HCV and GBV-B RdRps have specificity in RdRp–RNA interaction by using the template for the initiation of one viral RNA product and determining whether other viral RdRps will also recognize this RNA. The 3′ 121 nt of the HCV minus-strand RNA, named H121 (Fig. 8A), was required for HCV RNA synthesis in vitro and in the replicon system (Reigadas et al., 2001; Friebe et al., 2001). H121 was produced along with an RNA named +1G that is identical except for the initiation cytidylate. The HCV RdRp was able to recognize H121 and direct the synthesis of a product of the expected size (Fig. 8B and data not shown). Furthermore, efficient RNA synthesis requires a 3′-initiation cytidylate, as +1G was reduced more than fivefold for RNA synthesis in comparison to H121.

To examine the requirements for RNA synthesis from H121 further, we tested the effects of lowering the GTP concentration to 2 μM (Fig. 8B). Higher GTP concentration is required for de novo initiated RNA synthesis by the HCV RdRp from a number of templates (e.g., Luo et al., 2000; Kao et al., 2000; Zhong et al., 2000a; Ranjith-Kumar et al., 2002a). Decreasing the GTP concentration to 2 μM reduced RNA synthesis to background levels, demonstrating a special requirement for GTP, likely as the initiation nucleotide. These reactions were performed at 0.25 μM final concentration of ATP, indicating that a lower concentration of ATP is acceptable for RNA synthesis from H121. The BVDV and GBV RdRps were also able to direct RNA synthesis from H121 with the same requirements for the template initiation cytidylate and for GTP. These results are consistent with the results we had previously obtained with the

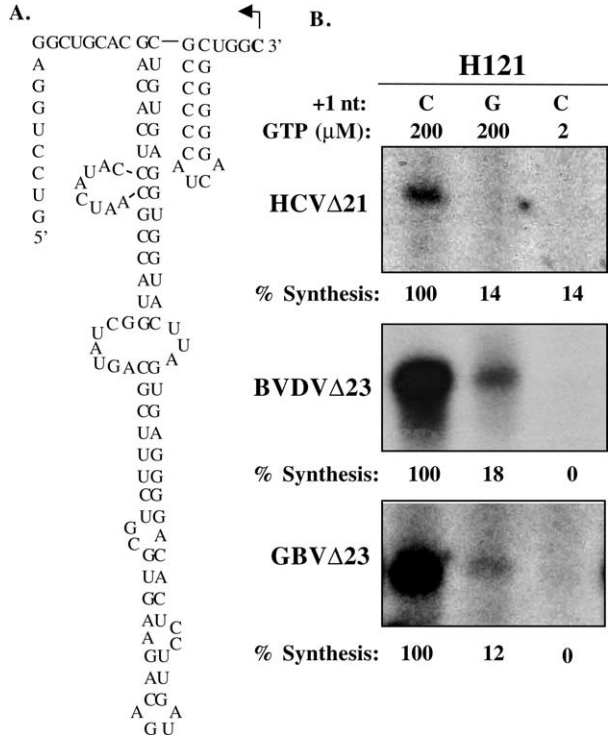

Fig. 8. Template specificity for RNA synthesis by recombinant RdRps. (A) Sequence and predicted secondary structure for the 3′-terminal 121 nucleotides of the HCV genome, named H121, as described by Schuster et al. (2003). The bent arrow denotes the initiation cytidylate. (B) RNA synthesis by the HCV, BVDV, and GBV RdRps using H121 or a version of H121 named +1G where the 3′-terminal initiation cytidylate is mutated to a guanylate. The percent synthesis is calculated from the autoradiogram shown, but is consistent in independently performed experiments.

HCV RdRp using minimal length templates (Ranjith-Kumar et al., 2002a,b). Furthermore, the fact that all three RdRps are capable of RNA synthesis from an HCV template indicates that the initiation site can provide specificity for RNA synthesis in vitro by recombinant RdRps (Fig. 8).

Effects of HCV RdRp inhibitors on the GBV RdRp

Given that there are several similarities and differences in the requirements for activities of the HCV and the GBV-B RdRps, we wanted to determine whether drugs that can inhibit the HCV RdRp can affect the GBV-B RdRp. Previously, a GTP analog with a ribose-2-hydroxyl and a 3′deoxy, named 3′ deoxyGTP, was shown to inhibit the HCV RdRp with an IC_{50} and an IC_{90} of 85 and 750 nM, respectively. Using the primer-extension assay, 3′ deoxyGTP had an IC_{50} of 550 nM for the GBV-B RdRp (Fig. 9). A benzo-1,2,4-thiadiazine compound, compound 4 ($C_{21}H_{21}N_3O_4S$), was recently characterized to inhibit RNA synthesis by the HCV RdRp in vitro with an IC_{50} of between 80 and 100 nM. In the cell-based replicon system, its IC_{50} was approximately 500 nM (Dhanak et al., 2002). Compound 4 was tested from 50 nM to 10 μM but did not affect the level of RNA synthesis by the GBV-B RdRp (Fig. 9). Thus, this nonnucleoside inhibitor is specific for the HCV RdRp.

Concluding comments

The GBV-B and HCV NS5B proteins share all of the activities determined thus far for the HCV RdRp, including the ability to extend from a primed template, initiate de novo (with specificity for the initiation nucleotide), generate products from two or more noncovalently linked templates, and add nontemplated nucleotides to the 3′-terminus of RNAs. All of the RdRps will recognize a template as long as it contains a proper initiation site. However, a number of details in each of the above activities are distinct for the HCV and GBV-B RdRps, including preferences for concentrations of divalent metal cofactors, differences in the frequency of template switch preferences, and nontemplated nucleotide addition.

The effect of divalent metals on the GBV-B and HCV RdRps are especially notable. The HCV RdRp strongly prefers Mn^{2+} for de novo initiation while Mg^{2+} was incapable of efficient de novo initiation. Mn^{2+} and Mg^{2+} were capable of supporting both primer-extension and de novo initiation by the GBV-B RdRp over a range of concentrations (Figs. 2A and 5). However, reactions with Mg^{2+} resulted in higher accumulation of both primer extension and de novo initiation products made by the GBV-B RdRp relative to Mn^{2+}. An unexpected feature of the effect of Mn^{2+} is that its effect is only observed with templates that are shorter than 15 nt, indicating that the effect of Mn^{2+} is at least partially to interact with the template RNA. This observation makes it unlikely that Mn^{2+} will stimulate RNA synthesis by GBV RdRp in the infected cell. Previ-

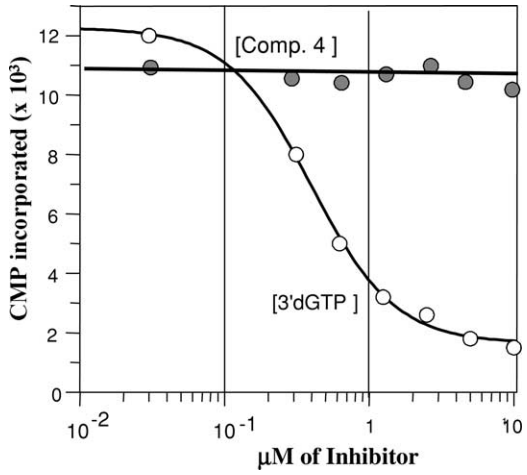

Fig. 9. Effects of two inhibitors of HCV RdRp on the GBV-B RdRp. The concentration of the compounds used is indicated on the horizontal axis in μM. The incorporation of radiolabeled CMP is shown on the vertical axis. 3′dGTP is an analog where the ribose 3′ is a deoxy, while the ribose 2′ contains a hydroxyl group. Compound 4 was characterized by Dhanak et al. (2002).

ously, Zhong et al. (2000b) reported that the GBV-B RdRp specifically requires Mn^{2+} and cannot use Mg^{2+} for RNA synthesis. Our results differ substantively from those of Zhong et al. (2000b). However, our results are consistent for a number of templates.

GBV-B infection of tamarins has been claimed to represent a potential surrogate model system to study HCV replication. In our studies, a compound that inhibits the HCV RdRp had no effect on the GBV-B RdRp. Together with the differences in the various activities we tested, it is more likely that small changes in one or a few amino acids in the NS5B can alter the specificity for substrates required for nucleotide polymerization and for targets for antivirals active against HCV. Nonetheless, the GBV-B RdRp could be useful as a system to demonstrate the specificity of a compound for evaluating RdRp inhibitors for HCV.

Materials and methods

Cloning, expression, and purification of GBV-B NS5B

Infectious cDNA for GBV-B was kindly provided by Drs. Jens Bukh and Robert Purcell at the National Institute of Allergy and Infectious Diseases at the National Institutes of Health. Primers were designed according to the published GBV-B sequence (Bukh et al., 1999). Additional sequences to encode an amino-terminal methionine and six carboxy-terminal histidines were engineered to facilitate cloning into pET-21b (Novagen). Production of soluble NS5B was induced by propagating recombinant *E. coli* in 1 mM isopropyl-thio-β-D-galactopyranoside (IPTG) at 25°C for 4 h. NaCl at 300 mM and glycerol at 10% helped to maintain the solubility of the recombinant protein. Soluble lysates were passed onto a Talon column (Clontech Inc., Palo Alto, CA); the column was extensively washed in buffer containing 300 mM NaCl and eluted with a gradient of imidazole up to 0.5 M. The peak of protein was dialyzed in a Tris buffer containing 0.15 M NaCl and purified over a poly(U)-agarose column (Pharmacia Inc.) and eluted with a gradient of increasing NaCl. To quantify NS5B, serially diluted sampled were electrophoresed on SDS–PAGE and scanned by densitometry relative to BSA standards. Proteins were then concentrated to approximately 1 mg/ml and stored in aliquots at −80°C.

RdRp assay

A primer-extension assay used a poly(rC):oligo(rG)-primed substrate with the following modifications. After the reaction was completed, 25 μl of stop buffer (containing 1× Dulbecco's phosphate-buffered saline (PBS) w/o $CaCl_2$, $MgCl_2$, and 0.1 M EDTA) was added and then the reaction mixture was transferred to Streptavidin FlashPlate (NEN Life Science, SMP103). After incubation for 1 h capture at room temperature, the plate was washed three times with 200 μl of 1× PBS with 0.5% Tween 20. It was then vacuum dried, and the signal was quantified by scintillation counting (Packard Inc.).

RNA synthesis assays using virally derived RNAs were previously described by Ranjith-Kumar et al. (2001). Standard RdRp assays consisted of 2.5 pmol of template LE21 with 50–100 ng of NS5B in 20 μL. The products were radiolabeled by the incorporation of [α-^{32}P]-CTP. Assessment of whether the GBV RdRp could synthesize a nascent RNA using more than one template (template switch) was performed as described in Kim and Kao (2001). The template used, dd(−)21, contains a 3′-most dideoxynucleotide to prevent ligation of the templates.

RNA synthesis from H121, the 3′ end of the HCV 1B genome, used [α-^{32}P]ATP (10 mCi/ml) as the radiolabel (CTP and UTP were present at >100 μM and GTP was at 200 μM). RNA synthesis with H121 is less efficient with [^{32}P]CTP, likely due to CTP being required during the formation of the first phosphodiester bond with H121 (Fig. 8A) (Reigadas et al., 2001). The sequence of H121 was derived from the information in Kashiwagi et al. (2002) and transcribed in vitro by annealing two partially overlapping DNA oligonucleotides and extending with the Taq DNA polymerase. The DNA oligonucleotide encoding the 5′ portion of H121 also contained a promoter for the T7 RNA polymerase. Transcripts corresponding to the correct length relative to molecular markers were excised from a 6% denaturing gel and eluted in 0.3 M ammonium acetate solution, checked for quantity and quality prior to use. A mutation at the 3′-terminal cytidylate was made using a single-nucleotide change in the DNA oligonucleotide encoding this position.

Circular dichroism (CD) spectroscopy

CD analysis was performed on purified HCV Δ21 NS5B and GBV-B Δ23 NS5B (0.3 mg/ml in 25 mM Tris pH 7.5, 25 mM KCl, 5 mM $MgCl_2$, and 0.4% dimethylsulfoxide) at 20°C. Far-UV CD spectra were recorded on a Jasco J-710 CD instrument using a 0.1-cm path-length cell. Ten spectral scans were accumulated using a time constant of 2 s with a 1 nM constant bandwidth at 50 nm/min. Thermal stability of the GBV-B NS5B was measured by scanning the sample at 220 nm, a wavelength suitable for monitoring α-helices. The sample is heated at a rate of 1°C/min. Thermal stability data were then analyzed using the computer program Grafit and a fitting equation adapted from Doyle and Hensley (1997) to predict the midpoint transition temperature (T_m).

Generation of polyclonal antisera

GBV-B NS5B synthetic peptides were selected by profiling hydrophobicity/antigenicity plots using the Genetics Computer Group sequence analysis software package (Univ. of Wisconsin). Peptides conjugated to keyhole limpet hemocyanin were provided by Multiple Peptide Systems

(San Diego, CA) and generated to the following oligopeptide from GBV-B NS5B: T_{228}PQKPTKKPPRLIS_{241}. Polyclonal antibodies to this peptide were made using two rabbits. Sequential bleeds were tested and the serum was used at 1:1000 dilution in Western blots.

Acknowledgments

We thank our colleagues at GlaxoSmithKline and Indiana University for helpful discussions and the NSF for funding the Kao Lab. C. Kao acknowledges a fellowship from the Linda and Jack Gill Foundation.

References

Alter, M.J., Mast, E.E., 1994. The epidemiology of viral hepatitis in the United States. Gastroenterol. Clin. N. Am. 23, 437–455.

Behrens, S.-E., Tomei, L., De Francesco, R., 1996. Identification and properties of the RNA-dependent RNA polymerase of hepatitis C virus. EMBO J. 15, 12–22.

Buck, K.W., 1996. Comparison of the replication of positive-strand RNA viruses of plants and animals. Adv. Virus Res. 47, 159–251.

Bukh, J., Apgar, C.L., Yanagi, M., 1999. Toward a surrogate model for hepatitis C virus: an infectious molecular clone of the GB virus-B hepatitis agent. Virology 262, 470–478.

Butkiewicz, N., Yao, N., Zhong, W., Wright-Minogue, J., Ingravallo, P., Zhang, R., Durkin, J., Strandring, D., Baroudy, B., Sangar, D., Lemon, S., Lau, J., Hong, Z., 2000. Virus-specific cofactor requirement and chimeric hepatitis C virus/GB virus B nonstructural protein 3. J. Virol. 74, 4291–4301.

De Francesco, R., Behrens, S.-E., Tomei, L., Altamura, S., Jiricny, J., 1996. RNA-dependent RNA polymerase of hepatitis C virus. Methods Enzymol. 275, 58–67.

Deinhardt, F., Holmes, A.W., Capps, R.B., Popper, H., 1967. Studies on the transmission of human viral hepatitis to marmoset monkeys. I. Transmission of disease, serial passages, and description of liver lesions. J. Exp. Med. 125, 673–688.

Dhanak, D., Duffy, K., Johnston, V.K., Lin-Goerke, J., Darcy, M., Shaw, A.N.G.B., Silverman, C., Gates, A.T., Earnshaw, D.L., Casper, D.J., Kaura, A., Baker, A., Greenwood, C., Gutshall, L.L., Maley, D., DelVecchio, A., Macarron, R., Hofmann, G.A., Alnoah, Z., Cheng, H.-Y., Chan, G., Khandekar, S., Keenan, R.M., Sarisky, R.T., 2002. Identification and biological characterization of heterocyclic inhibitors of the Hepatitis C virus RNA-dependent RNA polymerase. J. Biol. Chem. 277, 38322–38327.

Doyle, M., Hensley, P., 1997. Experimental dissection of protein-protein interactions in solution. Adv. Mol. Cell. Biol. 22A, 279–337.

Ferrari, E., Wright-Minogue, J., Fang, J., Baroudy, B., Lau, J., Hong, Z., 1999. Characterization of soluble hepatitis C virus RNA-dependent RNA polymerase expressed in *Escherichia coli*. J. Virol. 73, 1649–1654.

Friebe, P., Lohmann, V., Krieger, N., Bartenschlager, R., 2001. Sequences in the 5 untranslated region of the hepatitis C virus required for RNA replication. J. Virol. 75, 12047–12057.

Kao, C., Del Vecchio, A., Zhong, W., 1999. De novo initiation of RNA synthesis by a recombinant Flavivirus RNA-dependent RNA polymerase. Virology 253, 1–7.

Kao, C.C., 2002. Lessens learned from the core RNA promoters of Brome mosaic virus and Cucumber mosaic virus. Mol. Plant Pathol. 3, 53–59.

Kao, C.C., Ecker, D., Singh, P., 2001. De novo initiation of viral RNA-dependent RNA synthesis. Virology 287, 252–260.

Kao, C.C., Yang, X., Kline, A., Wang, Q.M., Barket, D., Heinz, B.A., 2000. Template requirements for RNA synthesis by a recombinant hepatitis C virus RNA-dependent RNA polymerase. J. Virol. 74, 11121–11128.

Kashiwagi, T., Hara, K., Kohara, M., Iwahashi, J., Hamada, N., Honda-Yoshino, H., Toyoda, T., 2002. Promoter/origin structure of the complementary strand of hepatitis C virus genome. J. Biol. Chem. 277, 28700–28705.

Kim, M.J., Zhang, W., Hong, Z., Kao, C.C., 2000. The bovine viral diarrhea virus RNA-dependent RNA polymerase recognizes different nucleotide moieties during de novo initiation and elongation of RNA synthesis. J. Virol. 74, 10312–10322.

Kim, M.-J., Kao, C., 2001. Factors regulating template switch in vitro by viral RNA-dependent RNA polymerases: implications for RNA-RNA recombination. Proc. Natl. Acad. Sci. USA 98, 4972–4977.

Lohmann, V., Korner, F., Herian, U., Bartenschlager, R., 1997. Biochemical properties of hepatitis C virus NS5B RNA-dependent RNA polymerase and identification of amino acid sequence motifs essential for enzymatic activity. J. Virol. 71, 8416–8428.

Lohmann, V., Roos, A., Korner, F., Koch, J., Bartenschlager, R., 1998. Biochemical and kinetic analyses of NS5B RNA-dependent RNA polymerase of the hepatitis C virus. Virology 249, 108–118.

Lohmann, V., Roos, A., Korner, F., Koch, J.O., Bartenschlager, R., 2000. Biochemical and structural analysis of the NS5B RNA-dependent RNA polymerase of the hepatitis C virus. J. Viral Hepat. 7, 167–174.

Luo, G., Hamatake, R.K., Mathis, D.M., Racela, J., Rigat, K.L., Lemm, J., Colonno, R.J., 2000. De novo initiation of RNA synthesis by the RNA-dependent RNA polymerase (NS5B) of hepatitis C virus. J. Virol. 74, 851–863.

Muerhoff, A.S., Leary, T.P., Simons, J.N., Pilot-Matias, T.J., Dawson, G.J., Erker, J.C., Chalmers, M.L., Schlauder, G.G., Desai, S.M., Mushahwar, I.K., 1995. Genomic organization of GB viruses A and B, two new members of the Flaviridae associated with GB agent hepatitis. J. Virol. 69, 5621–5630.

Oh, J.-W., Sheu, G.-T., Lai, M.M., 2000. Template requirements and initiation site selection by hepatitis C virus polymerase on a minimal viral RNA template. J. Biol. Chem. 275, 17710–17717.

Ranjith-Kumar, C.T., Gajewski, J.G.L., Maley, D., Sarisky, R.T., Kao, C.C., 2001. Terminal nucleotidyl transferase activity of recombinant flaviviridae RNA-dependent RNA polymerases: implication for viral RNA synthesis. J. Virol. 75, 8615–8623.

Ranjith-Kumar, C.T., Gutshall, L., Kim, M.-J., Sarisky, R.T., Kao, C.C., 2002a. Requirements for de novo initiation of RNA synthesis by recombinant Flaviviridae RNA-dependent RNA polymerase. J. Virol. 76, 12526–12536.

Ranjith-Kumar, C.T., Kim, Y.C., Gutshall, L., Silverman, C., Khandekar, S., Sarisky, R.T., Kao, C.C., 2002b. Mechanism of de novo initiation by the hepatitis C virus RNA-dependent RNA polymerase: role of divalent metals. J. Virol. 76, 12513–12525.

Reigadas, S., Ventura, M., Sarih-Cottin, L., Castroviejo, M., Litvak, S., Astier-Gin, T., 2001. HCV RNA-dependent RNA polymerase replicates in vitro the 3 terminal region of the minus-strand RNA more efficiently than the 3 terminal region of the plus-strand RNA. Eur. J. Biochem. 268, 5857–5867.

Schaluder, G., Dawson, G., Simons, J., 1995a. Molecular and serologic analysis in the transmission of the GB hepatitis agents. J. Med. Virol. 46, 81–90.

Schaluder, G., Pilot-Matias, T.J., Gabriel, G.S., 1995b. Origin of GB-hepatitis viruses. Lancet 346, 447–448.

Schuster, C., Isel, C., Imbert, I., Ehresmann, C., Marquet, R., Kieny, M.P., 2003. Secondary structure of the 3 terminus of hepatitis C virus minus-strand RNA. J. Virol. 76, 8058–8068.

Shim, J.H., Larson, G., Wu, J.Z., Hong, Z., 2002. Selection of 3′-template bases and initiating nucleotides by hepatitis C virus NS5B RNA-dependent RNA polymerase. J. Virol. 76, 7030–7039.

Simons, J.N., Pilot-Matias, T.J., Leary, T.P., 1995. Identification of two flavivirus-like genomes in the GB hepatitis agent. Proc. Natl. Acad. Sci. USA 92, 3401–3405.

Wang, Q.M., Hockman, M.A., Staschke, K., Johnson, R.B., Case, K.A., Lu, J., Parsons, S., Zhang, F., Rathnachalam, R., Kirkegaard, K., Colacino, J.M., 2002. Oligomerization and cooperative RNA synthesis activity of hepatitis C virus RNA-dependent RNA polymerase. J. Virol. 76, 3865–3872.

World Health Organization. 1998. Lancet 351, 1415.

Zhong, W., Ferrari, E., Lesburg, C.A., Maag, D., Ghosh, S.K., Cameron, C.E., Lau, J.Y., Hong, Z., 2000a. Template/primer requirements and single nucleotide incorporation by hepatitis C virus nonstructural protein 5B polymerase. J. Virol. 74, 9134–9143.

Zhong, W., Gutshall, L., Del Vecchio, A., 1998. Identification and characterization of an RNA-dependent RNA polymerase activity within the nonstructural protein 5B of bovine viral diarrhea virus. J. Virol. 72, 9365–9369.

Zhong, W., Ingravallo, P., Wright-Minogue, J., Uss, A., Skelton, A., Ferrari, E., Lau, J., Hong, Z., 2000b. RNA-dependent RNA polymerase activity encoded by GB virus-B non-structural protein 5B. J. Viral Hepat. 7, 335–342.